Наносистеми, наноматеріали, нанотехнології
Nanosistemi, Nanomateriali, Nanotehnologii
2025, т. 23, № 4, сс. 1015–1028
https://doi.org/10.15407/nnn.23.04.1015

PACS numbers: 31.15.es, 61.05.cp, 61.48.-c, 68.37.Hk, 68.55.ap, 81.05.ub, 81.05.uj

Investigation of the Mechanism of Interaction Between Carbon Nanomaterial Particles and Nickel Ions

V. V. Tytarenko[1] and V. A. Zabludovsky[2]

[1]*Dnipro University of Technology,*
19, Dmytra Yavornytskoho Ave.,
UA-49005 Dnipro, Ukraine
[2]*Ukrainian State University of Science and Technologies,*
2, Lazaryana Str.,
UA-49010 Dnipro, Ukraine

In order to investigate a co-deposition mechanism of metal ions and ultradispersed diamond (UDD) particles or molecule fullerene C_{60}, the authors propose quantum-mechanical models for formation of metal–carbon complex. Adsorption properties of the nickel atoms on surface of UDD particles or C_{60}-fullerene molecule are studied by density functional theory method using the B3LYP hybrid functional. Models of complexes of UDD or C_{60}-fullerene molecule with one, two, and three bound metal ions are proposed and optimized. Calculations of complexes' total energies in the condensed state are carried out using the Gaussian 16 program package. Obtained results for the binding energy of adsorbed nickel ions with nanodiamond particle or C_{60}-fullerene molecule prove that adsorption of nickel ions on a surface of UDD particle or C_{60}-fullerene molecule from the aqueous solution of electrolytes is possible with formation of stable metal–carbon-complexes' nanomaterial. As assumed, the formed metal–carbon complexes, because of the adsorption of metal atoms on the surface of UDD particle or C_{60}-fullerene molecule, gain a charge in the electrolyte solution and move towards the cathode under the action of an electric field created by the potential difference between the anode and the cathode. Phase composition analyses for metal coatings, the results of SEM studies of the surface, and metallography of end sections of electrolytic nickel coatings confirm the assumption about the mechanism of co-deposition of metal ions and UDD or C_{60}-fullerene molecule on the cathode. The presence of carbon-containing material in the composite nickel coating is recorded as dark inclusions.

Для дослідження механізму спільного осадження йонів металів і частинок ультрадисперсних діямантів (УДД) або молекул фуллерену C_{60} автори запропонували квантово-механічні моделі утворення метал-

вуглецевого комплексу. Адсорбційні властивості атомів Ni на поверхні частинок УДД або молекули фуллерену C_{60} досліджуються методом теорії функціоналу густини з використанням гібридного функціоналу B3LYP. Запропоновано й оптимізовано моделі комплексів УДД або молекули фуллерену C_{60} з одним, двома та трьома зв'язаними йонами металу. Розрахунки повних енергій комплексів у конденсованому стані проведено за допомогою програмного пакету Gaussian 16. Одержані результати щодо енергії зв'язку адсорбованих йонів Ni з частинкою нанодіяманту або молекулою фуллерену C_{60} довели, що адсорбція йонів Ni на поверхні частинок УДД або молекули фуллерену C_{60} з водного розчину електролітів можлива з утворенням стабільного наноматеріялу з метал-вуглецевих комплексів. Можна припустити, що утворені метал-вуглецеві комплекси в результаті адсорбції атомів металу на поверхні частинки УДД або молекули фуллерену C_{60} набувають заряду в розчині електроліту та рухаються до катоди під дією електричного поля, створеного ріжницею потенціялів між анодою та катодою. Аналізи фазового складу металевих покриттів, результати СЕМ-досліджень поверхні та металографія торцевих ділянок електролітичних ніклевих покриттів підтверджують припущення про механізм спільного осадження йонів металу й УДД або молекули фуллерену C_{60} на катоді. Присутність карбонвмісного матеріялу в композитному ніклевому покритті фіксується у вигляді темних включень.

Key words: electrodeposition, carbon nanomaterial, metal–carbon complex, quantum-mechanical model, binding energy.

Ключові слова: електроосадження, вуглецевий наноматеріял, металокарбоновий комплекс, квантово-механічний модель, енергія зв'язку.

(Received 21 February, 2025)

1. INTRODUCTION

Creation of composite electrolytic coatings (CEP) is one of the topical directions of solid-state physics. The principle of preparation of CEP is based on the fact that dispersed phase particles are co-precipitated together with metals from aqueous electrolyte solutions. Being included into coatings, the particles significantly improve their operational properties (hardness, wear resistance, corrosion resistance) and give them new qualities (antifriction, magnetic, catalytic) [1–6]. Due to their excellent mechanical properties, including high strength, high ductility and low density, nanocarbons such as graphene, fullerene, carbon nanotubes, and ultradispersed diamonds (UDD) have become potential strengthening elements in metal-matrix composites. This ensured that metal-matrix composites are widely used in various industries, and the development of new types of composite coatings and the search for ways to control their properties is an important scientific and applied task.

The efficiency of the use of CEP is largely determined by the nature of the dispersed phase. Of particular interest as modifiers of composite electroplating coatings are UDD particles, which belong to the class of superhard materials [7–11]. In addition, a promising dispersed material for composite coatings is C_{60}-fullerene, which has a whole complex of unique chemical properties [12–14].

The unique physical and chemical properties of electrodeposited metal films depend largely on the concentration of carbon nanomaterial particles (CNPs) in the metal matrix. Therefore, the control and management of the content of CNPs in composite metal films has recently received special attention. The solution to such a problem is impossible without studying the mechanism of structure formation of carbon-containing composite metal coatings.

In recent years, a large amount of research has been focused on the technology of obtaining and the mechanical properties of metal-based composites reinforced with graphite and/or carbon nanotubes (CNTs) [15–18]. Due to the complex composite structures and interfacial microstructures, there are great difficulties in determining the structure–property relationships at the microlevel using experimental approaches. At the same time, nanocarbon/metal interfaces are also important for the mechanical performance of nanocarbon-reinforced composites. Dislocations can be inhibited at grain boundaries or interfaces, and external loads can be transferred near the interfaces from metal to nanocarbon, leading to strengthening effects of the metal matrix [19].

Atomic-scale modelling, including first principles, is suitable for investigating the structure–property relationships of nanocarbon-reinforced metal-matrix composites at the microscale. In recent years, the development of methods of quantum mechanics, quantum chemistry, computational techniques and appropriate software makes it possible to calculate the binding energy in metal clusters, thus, increasing the number of research works on atomic-scale modelling of composite carbon-containing materials. Thus, the works [20–24] consider the structural models of nanocarbon–metal interfaces constructed by stacking graphite (Gr) or CNTs in a metal matrix. To evaluate the interfacial bonding of Gr–metal and CNT–metal interfaces, bonding energies have been calculated using the density functional theory (DFT) method. As shown, the value of the binding energy of Ni atoms adsorbed on the Gr surface varies from 0.037 eV [23] to 0.133 eV [24]. However, these calculations were carried out for adsorption of atoms in vacuum. To describe the mechanism of co-precipitation in aqueous electrolyte solution of metal ions and CNPs on the cathode, it is necessary to consider structural models consisting of CNPs and positively charged metal ions.

In order to establish the mechanism of transfer of CNPs in the

volume of electrolytic bath and the process of co-precipitation of metal ions with UDD particles or fullerenes on the cathode, this work proposes a mathematical model of metal–carbon complex formation based on the results of calculation of binding energy.

2. MATERIALS AND METHODS

Electrodeposition of composite coatings was carried out from sulphate nickel-plating electrolyte of the following composition: 300 g/l of $NiSO_4 \cdot 7H_2O$, 30 g/l of H_3BO_3, 50 g/l of $Na_2SO_4 \cdot 10H_2O$, at pH of 5. The concentration of UDD or C_{60}-fullerene in the aqueous electrolyte solution was of 2 g/l. Electrodeposition was carried using a direct current at a density of 1 A/dm^2.

The polarization dependences were recorded in the potentiodynamic mode on a P-5827M potentiostat at a potential sweep rate of 10 mV/s. The measurements were carried out in a three-electrode electrolytic cell. A copper plate was used as the working electrode (cathode). The reference electrode was a silver-chloride electrode, and the auxiliary electrode was a platinum electrode.

X-ray microanalysis was performed using a JSM-64901LV scanning electron microscope (Japan). X-ray phase analysis of the films was conducted on a DRON-2.0 diffractometer using scintillation detection of x-rays. Shooting to determine the phase composition of nickel films was carried out in monochromatic Cu and Co$K\alpha$ radiation.

The end sections for metallographic studies were mechanically polished using optical microscope MIM-8. To reveal the cross-sectional structure, the coatings were etched in 50% nitric-acid solution for 10–15 s.

In order to establish the possibility of Ni^{2+}-ions' adsorption on the surface of UDD or fullerene in an aqueous electrolyte solution and the formation of stable positively charged complexes, this work considers a model problem, which investigates the interaction of Ni ions with the crystal-lattice cell of diamond, corresponding to the point symmetry group $m3m$ ($4/m\,{-}3\,2/m$), and a C60-fullerene molecule.

Some model approximations have been considered in order to calculate the binding energy of metal ions with CNPs.

1. Adsorption occurs in electrolyte solutions, in particular, in aqueous solutions, which requires the choice of a solvent model. Polarizable continuum model (PCM) [25] has been used as a solvation model.

2. Complexes obtained by an adsorption of metal ions on the surface of the CNPs must have a charge of an original metal ion due to the law of charge conservation.

3. Adsorption of metal ions on a surface of CNPs occurs alternately. Each subsequent metal ion is adsorbed on a CNP, which already has a charge obtained by the previous adsorption.

Calculations of the binding energy of adsorbed nickel ions with the lattice cell of diamond and C_{60} fullerene were carried out using the DFT, which has recently firmly taken the place of one of the most popular methods for calculating the electronic structure of atoms, molecules, clusters, solids, *etc.* [26, 27]. The growing popularity of DFT is due, first of all, to the combination of a sufficiently high accuracy of the obtained results, competing, in some cases, with the accuracy of *ab initio* methods of electron-correlations' record, and to rather moderate requirements for computational resources, allowing to carry out calculations of the systems consisting of hundreds of atoms and being of interest for modern nanotechnology [28]. In addition, the DFT method has been used to investigate the adsorption characteristics of transition metals [29–31].

The choice of the basis set has been based on the fact that the calculation of energy quantities had been performed for metal, for which the interaction of valence electrons plays the most important role. In order to describe such interactions, valence-split basis set have been used. Basis set extended 6-31-G(*d*), which contains *d*-type atomic orbitals for taking into account polarization of metals' electron density, have been used to describe the interactions in many-electron systems. Calculations of complexes' total energies and their structures in the condensed state have been carried out using the Gaussian 16 program package [32]. The temperature and the pressure have been chosen as 295 K and 105 Pa, respectively. The most suitable for calculations of structural and thermochemical characteristics of metal complexes is the three-parameter B3LYP hybrid functional [33–35]. It should be taken into account that, in the problem posed in this work, not absolute values of energies are used, but their difference values.

3. RESULTS AND DISCUSSION

The analysis of cathodic polarization curves (Fig. 1) showed that the presence of dispersed particles in the aqueous electrolyte solution leads to a shift of the cathode potential to the electronegative region that indicates an increase in the charge-transfer resistance. It can be assumed that the CNPs move towards the cathode surface due to adsorption of metal cations on their surface. Based on the solution of the Nernst–Planck equation, the results of the study of the elemental composition of coatings and the estimation of the concentration of dispersed phase in the coating, we proposed in Ref. [36] a mathematical model that describes the kinetics of the cathodic process of joint electrolytic deposition of metal ions and UDD particles. Analysis of the results of calculations [36] showed that the main factor affecting the transport of CNPs in the aqueous electrolyte solution is the potential gradient, and the

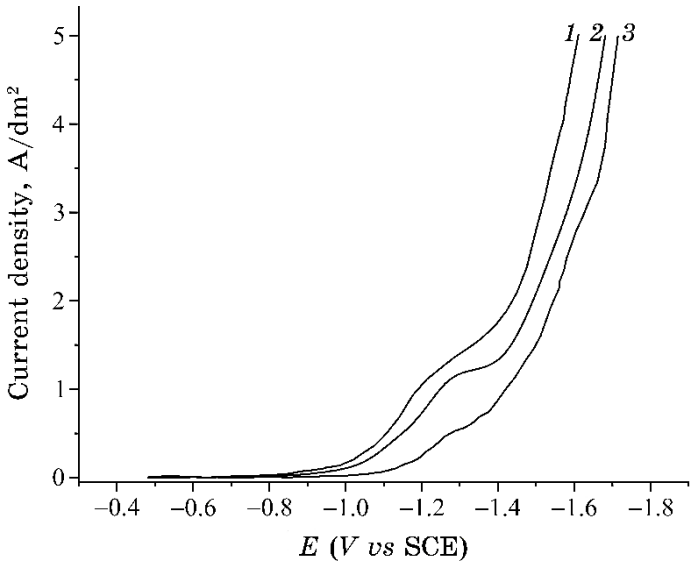

Fig. 1. Cathodic polarization–E curves obtained for hydrosulphate-nickel plating electrolyte: (*1*) without CNPs, (*2*) with presence of C_{60} fullerene, and (*3*) with presence of UDD.

contribution of the concentration gradient to the particle-flux density is insignificant.

Consequently, the transport of CNPs occurs mainly under the action of electric field rather than by diffusion mechanism. It can be assumed that the formed CNP–Me^{2+} complexes, as a result of adsorption of metal atoms on the surface of the CNP, acquire a charge in the electrolyte solution and move to the cathode under the action of the electric field created by the potential difference between the anode and the cathode.

To investigate the adsorption properties of nickel atoms on the surface of CNPs, we used the density functional theory method. In the considered model problem, the binding energy (ΔW) of an adsorbed metal ion with a diamond cell (Fig. 2) or with a C_{60}-fullerene molecule (Fig. 3) was determined as the difference between the total energy of the metal ion–CNP compound ($W_{C+Me^{2+}}$) and the sum of the energies of its constituent parts (W_C, $W_{Me^{2+}}$):

$$\Delta W = \left| W_{C+Me^{2+}} - (W_C + W_{Me^{2+}}) \right|, \qquad (1)$$

where W_C is the CNP energy, $W_{Me^{2+}}$ is the metal-ion energy.

In the case of alternate adsorption of metal ions, the binding en-

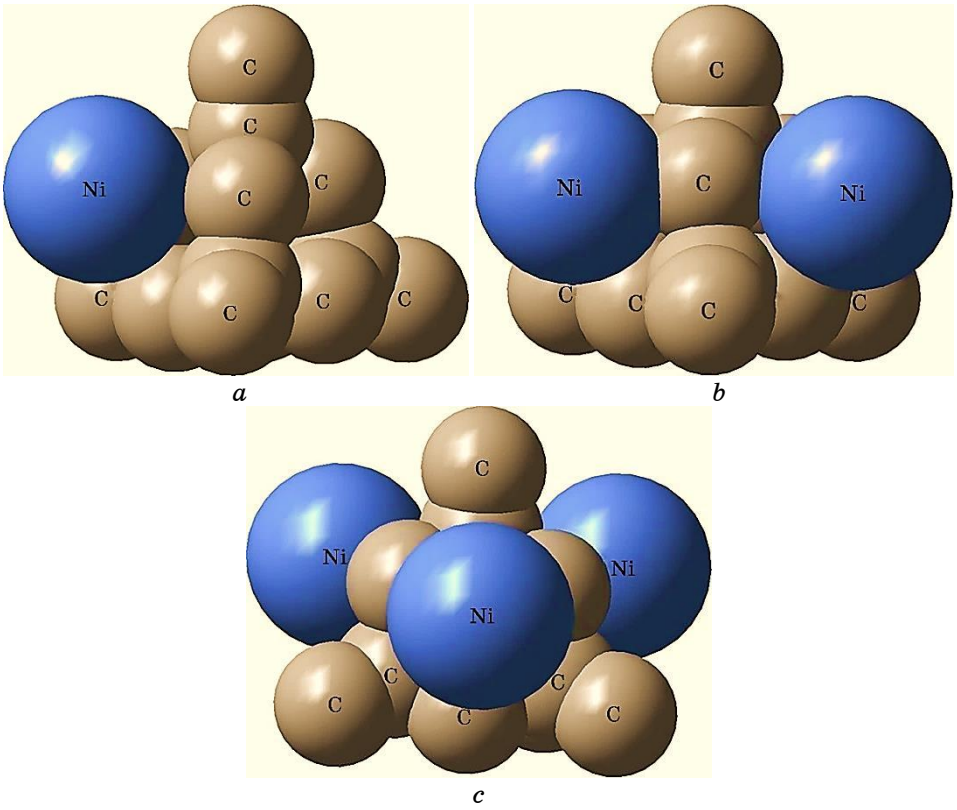

Fig. 2. Location of adsorbed nickel ions on the surface of the diamond cell: (*a*) diamond cell–Ni^{2+} compound, (*b*) diamond cell–$2Ni^{2+}$ compound, and (*c*) diamond cell–$3Ni^{2+}$ compound.

ergy to the CNP was calculated as the difference between the total energy of the CNP compound with one ($W_{C+Me^{2+}}$), two ($W_{C+2Me^{2+}}$) or three ($W_{C+3Me^{2+}}$) adsorbed metal ions and the energies of its constituent parts, respectively:
the energy of the CNP (W_C) and the energy of 1 metal ion ($W_{Me^{2+}}$),

$$\Delta W_1 = W_{C+Me^{2+}} - (W_C + W_{Me^{2+}}); \quad (2)$$

the energy of the CNP with 1 adsorbed metal ion ($W_{C+3Me^{2+}}$) and the energy of 1 metal ion ($W_{Me^{2+}}$),

$$\Delta W_2 = W_{C+2Me^{2+}} - (W_{C+Me^{2+}} + W_{Me^{2+}}); \quad (3)$$

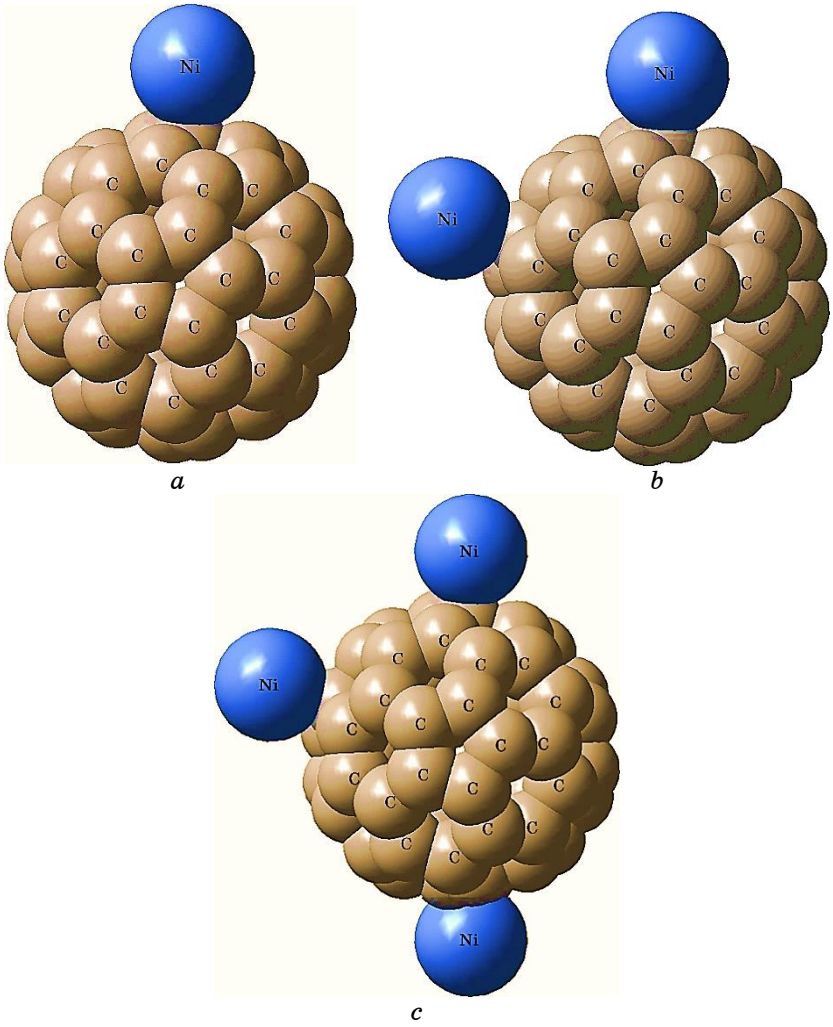

Fig. 3. Location of adsorbed nickel ions on the surface of the C_{60} fullerene: (*a*) C_{60}-fullerene–Ni^{2+} compound; (*b*) C_{60}-fullerene–$2Ni^{2+}$ compound, and (*c*) C_{60}-fullerene–$3Ni^{2+}$ compound.

the energy of the CNP with 2 adsorbed metal ions ($W_{C+2Me^{2+}}$) and the energy of 1 metal ion ($W_{Me^{2+}}$),

$$\Delta W_3 = W_{C+3Me^{2+}} - (W_{C+2Me^{2+}} + W_{Me^{2+}}). \quad (4)$$

UDD–Ni and C_{60}–Ni complexes were visualized using GaussView6 program package. For a clear representation of the model of the

TABLE. Binding energies of UDD–Ni and C_{60}–Ni complexes depending on the number of nickel ions adsorbed.

ΔW, eV	CNP	Number of Ni ions adsorbed (ion charge)		
		1 (+2*e*)	2 (+4*e*)	3 (+6*e*)
	C_{60} fullerene	1.907	1.582	0.240
	UDD	0.200	0.126	–0.114

CNP–nickel ion compound, covalent radii were chosen in Fig. 2 and Fig. 3. The interatomic distances in the diamond cell and C_{60} fullerene correspond to the experimental ones.

Since the surface of CNPs is large enough to host more than one metal ion, we have taken into consideration models, when one nanoparticle binds up to three metal ions.

According to 2nd approximation from computational details in Sec. 2, with addition of each new metal ion, the charge of the system should increase on 2*e* (*e* is the elementary electric charge). Models of complexes with 1 (Fig. 2, *a* and 3, *a*), 2 (Fig. 2, *b* and 3, *b*), or 3 (Fig. 2, *c* and 3, *c*) bound metal ions, which have charges of +2*e*, +4*e*, and +6*e*, respectively, have been proposed and optimized. The results of calculation of binding energy (ΔW [eV]) of adsorbed nickel ions with CNPs are given in Table.

From the calculation results shown in Table, it can be seen that, with the sequential addition of several metal ions, the binding energy with the CNP decreases. One and two nickel ions are firmly bound to the CNP, since their binding energy is much higher than the thermal-motion energy of 0.025 eV. A charge of +6*e* or more is not retained on the UDD particle.

Comparisons of the obtained values of the binding energy of the CNP–metal ion compound with the energy of thermal motion show that, in the aqueous electrolyte solution, adsorption of Ni^{2+} ions on the surface of CNP with the formation of stable CNP–Ni^{2+} complexes is possible. Consequently, the transfer of CNPs from the volume of aqueous electrolyte solution to the cathode surface is possible due to the acquisition of a positive charge by the CNP–Ni^{2+} complex.

To establish the presence of CNPs in the metal film, x-ray phase analysis of composite electrolytic coatings was carried out.

XRD patterns of composite metal–CNP films based on nickel is illustrated in Fig. 4, *a* and Fig. 5, *a*.

For comparison diffraction pattern of the one of pure nickel, the C_{60} fullerene and the UDD powder without impurities are illustrated on Fig. 4, *b*, *c* and Fig. 5, *b*, respectively. XRD patterns of Ni–C_{60} composite film, Ni–UDD composite film, and pure nickel have five characteristic peaks 2.03Ni, 1.26Ni, 1.24Ni, 1.06Ni, and 1.01Ni,

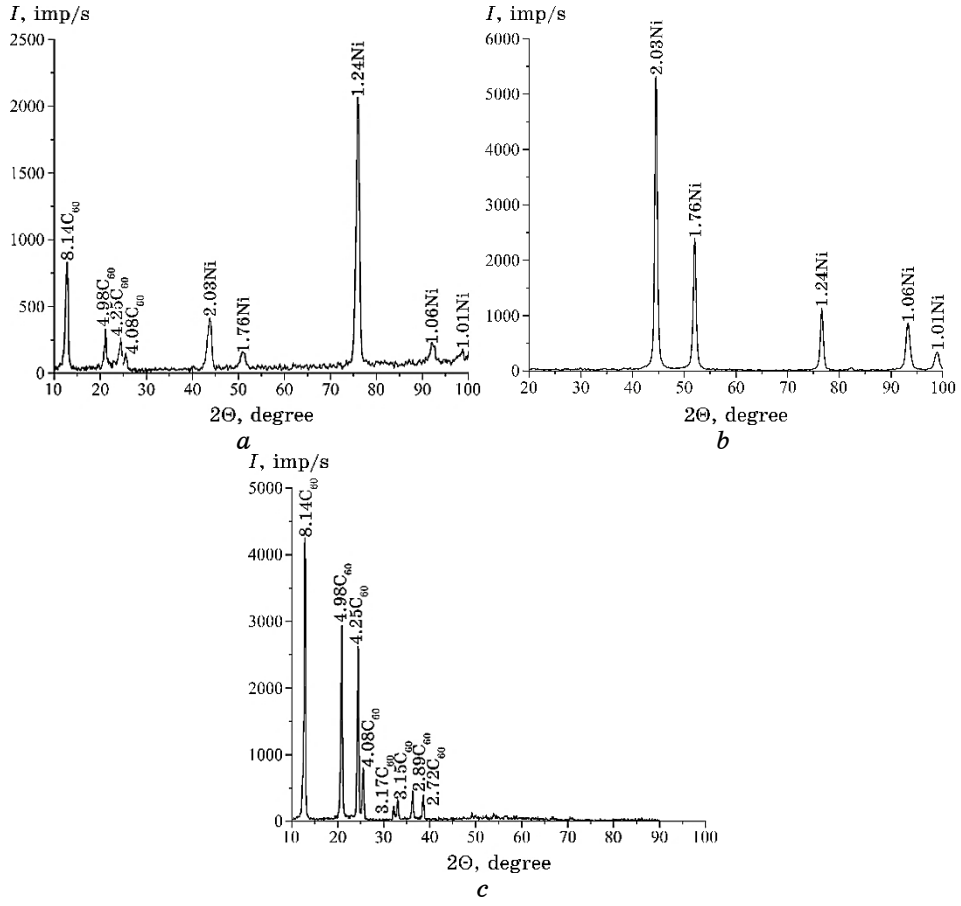

Fig. 4. XRD patterns of Ni–C_{60} composite film (*a*), nickel (*b*), C_{60} fullerene (*c*).

which are corresponding to Miller indices (111), (200), (220), (311), (222), respectively. However, intensities of these peaks are varying significantly. In case of pure nickel (Fig. 4, *b*), intensity distribution is close to reference one. Maxima intensity corresponds to (111) reflection that follows Bravais rule. Meanwhile, XRD patterns of Ni–C_{60} (Fig. 4, *a*) and Ni–UDD (Fig. 5, *a*) composite films have the highest intensity peak corresponding to (220) reflection.

Presumably, CNPs are blocking the active surface of the film preventing the further growth and giving the way for new centres of nucleation to appear. Faces, which are parallel to internal planes with the minimal speed of growth (111), are the most prominent in case of equilibrium crystallization, while, during a nucleation process, the most common directions are the ones with high indices. That explains redistribution of XRD-peaks' intensities.

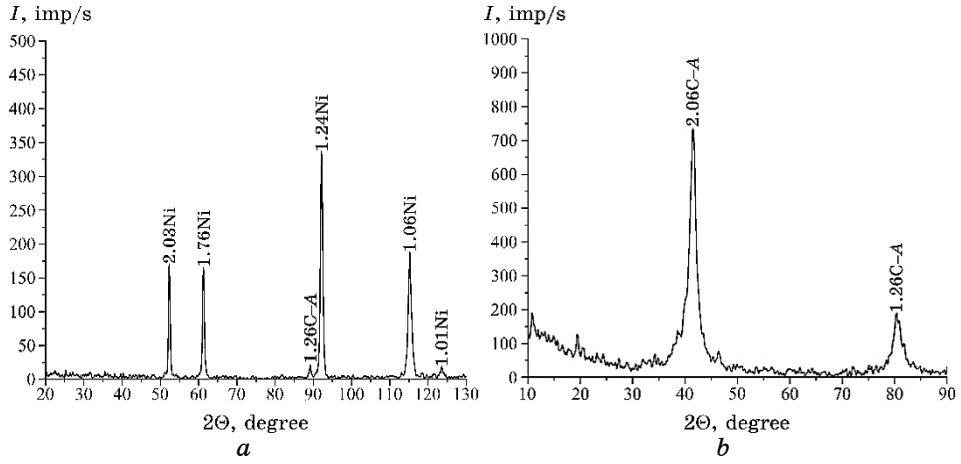

Fig. 5. XRD pattern for Ni–UDD composite film (*a*) and UDD (*b*).

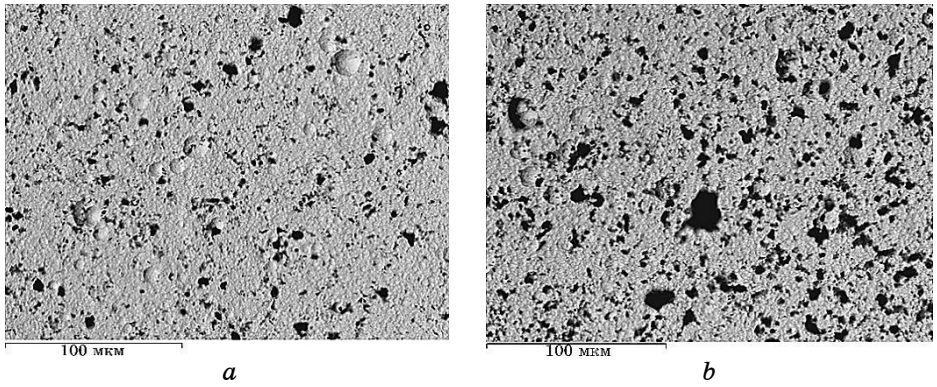

Fig. 6. SEM microphotographs of the composite nickel-coating surface: (*a*) Ni–UDD and (*b*) Ni–C_{60}.

SEM micrographs (Fig. 6) show images of the surfaces of composite electrolytic nickel coatings containing inclusions of UDD particles with a concentration of 1.71 wt.% (Fig. 6, *a*) and C_{60} fullerene with a concentration of 1.43 wt.% (Fig. 6, *b*). The main amount of CNPs in the coatings is recorded as dark inclusions.

Inclusion of CNPs in the coating composition complicates the surface diffusion of metal adatoms and prevents the growth of crystalline-phase nuclei, as a result of which the composite coatings are formed more fine-grained (crystallite size decreases from 104 nm for pure nickel to 80–85 nm for composite nickel coating), and the coating growth structure in the cross-section changes from columnar structure (Fig. 7, *a*) to microlayered one (Fig. 7, *b*, *c*).

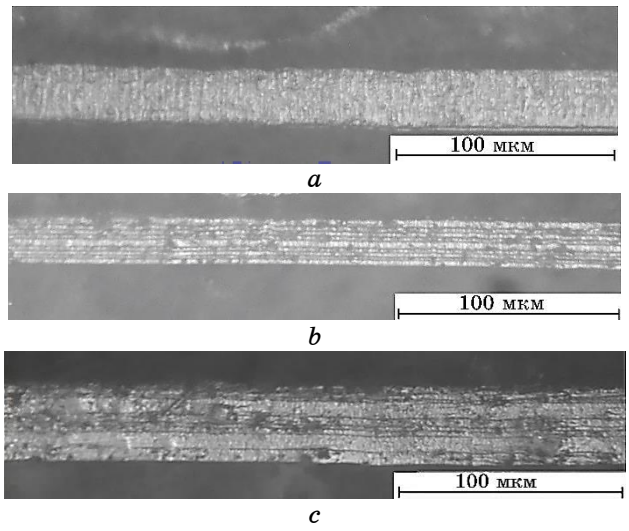

Fig. 7. Cross-sectional structure of electrolytic coatings: (*a*) nickel coating, (*b*) composite nickel coating Ni–UDD, (*c*) composite nickel coating Ni–C_{60}.

In microphotographs of CEP sections (Fig. 7, *b*, *c*), light layers of predominantly nickel with minimal content of CNPs' inclusions alternate with dark layers enriched with CNPs.

4. CONCLUSIONS

The proposed quantum-mechanical models of interaction of nickel ions with the diamond lattice cell corresponding to the point symmetry group $m3m$ ($4/m\,\bar{3}\,2/m$) and C_{60} fullerene have shown the possibility of Ni^{2+} ions adsorption on the surface of CNP in aqueous electrolyte solution with the formation of stable CNP–Ni^{2+} complexes. The transfer of CNPs from the volume of aqueous electrolyte solution to the cathode surface is possible due to the acquisition of a positive charge by the CNP–Ni^{2+} complex.

The increase in the cathode overpotential indicates a decrease in the area of the active surface of the cathode because of co-precipitation of CNPs, the transfer of which in the aqueous electrolyte solution is carried out under the action of the electric field. Studies of the phase composition of composite metal films show the presence of CNPs in the metal matrix. The formation of axial texture with large crystallographic indices is explained by the increase of cathodic overpotential, when UDD or C_{60}-fullerene particles are added to the aqueous electrolyte solution. UDD particles, reaching the cathode surface, block the growth of crystalline-phase nuclei

that leads to the formation of a more close-packed coating and changes the growth structure in the cross-section from columnar structure to microlayered one.

REFERENCES

1. G. K. Burkat, T. Fujimura, V. Yu. Dolmatov, E. A. Orlova, and M. V. Veretennikova, *Diam. Relat. Mater.*, **14**: 1761 (2005); https://doi.org/10.1016/j.diamond.2005.08.004
2. M. Liu, H. Liu, D. Wang, B. Liu, Y. Shi, F. Li, Y. Gong, L. Li, and W. Zhang, *Materials*, **12**, No. 2: 1105 (2019); https://doi.org/10.3390/ma12071105
3. W. Liping, G. Yan, X. Qunji, H. Liu, and T. Xu, *Mater. Sci. Eng. A*, **390**: 313 (2005); https://doi.org/10.1016/j.msea.2004.08.033
4. V. P. Isakov, A. I. Lyamkin, D. N. Nikitin, A. S. Shalimova, and A. V. Solntsev, *Protec. Met. Phys. Chem. Surf.*, **46**, No. 5: 578 (2010); https://doi.org/10.1134/S2070205110050138
5. V. V. Tytarenko, V. A. Zabludovsky, and E. Ph. Shtapenko, *Inorg. Mater.: Appl. Res.*, **10**, No. 3: 589 (2019); https://doi.org/10.1134/S2075113319030419
6. I. R. Robiul, Md. Hasan Ali, Md. Abu Jafor, and Md. Mahmodul Alam, *Mat. Sci.*, **6**, No. 5: 756 (2019); https://doi.org/10.3934/matersci.2019.5.756
7. V. A. Zabludovsky, V. V. Tytarenko, and E. Ph. Shtapenko, *Transactions of the IMF*, **95**, No. 6: 337 (2017); https://doi.org/10.1080/00202967.2017.1355463
8. Hiroshi Matsubara, Yoshihiro Abe, Yoshiyuki Chiba, Hiroshi Nishiyama, Nobuo Saito, Kazunori Hodouchi, and Yasunobu Inoue, *Electrochim. Acta*, **52**: Iss. 9: 3047 (2007); https://doi.org/10.1016/j.electacta.2006.09.043
9. Xiangzhu He, Yongxiu Wang, Xin Sun, and Liyong Huang, *Nanosci. Nanotechnol. Lett.*, **4**: 48 (2012); https://doi.org/10.1166/nnl.2012.1286
10. V. V. Tytarenko, V. A. Zabludovsky, E. Ph. Shtapenko, and I. V. Tytarenko, *Galvanotechnik*, **4**: 648 (2019).
11. C. Gheorghies, D. E. Rusu, and A. S. Bund, *Appl. Nanosci.*, **4**: 1021 (2014); https://doi.org/10.1007/s13204-014-0332-3
12. V. N. Tseluikin, *Prot. Met. Phys. Chem. Surf.*, **53**: 433 (2017); https://doi.org/10.1134/S2070205117030248
13. V. N. Tseluikin, O. G. Nevernaya, and G. V. Tseluikina, *Inorg. Mater.: Appl. Res.*, **2**: 521 (2011); https://doi.org/10.1134/S2075113311050297
14. X. Wang, F. Tang, X. Qi, Z. Lin, D. Battocchi, and X. Chen, *Nanomaterials*, **9**: 1476 (2019); https://doi.org/10.3390/nano9101476
15. A. Ramanathan, P. K. Krishnan, and R. Muraliraja, *Manuf. Process.*, **42**: 213 (2019); https://doi.org/10.1016/j.jmapro.2019.04.017
16. A. Dorri Moghadam, E. Omrani, P. L. Menezes, and P. K. Rohatgi, *Compos. Part B: Eng.*, **77**: 402 (2015); https://doi.org/10.1016/j.compositesb.2015.03.014
17. S. R. Bakshi, D. Lahiri, and A. Agarwal, *Int. Mater. Rev.*, **55**, No. 1: 41 (2013); https://doi.org/10.1179/095066009x12572530170543
18. Z. Hu, G. Tong, D. Lin, C. Chen, H. Guo, J. Xu, and L. Zhou, *Mat. Sci. Technol.*, **32**, No. 9: 930 (2016); https://doi.org/10.1080/02670836.2015.1104018
19. S. B. Sinnott and E. C. Dickey, *Mat. Sci. Eng. R*, **43**: 1 (2003); https://doi.org/10.1016/j.mser.2003.09.001
20. Caihao Qiu, Yishi Su, Jingyu Yang, Boyang Chen, Qiubao Ouyang, and Di Zhang, *Composites Part C: Open Access*, **4**: 100120 (2021);

https://doi.org/10.1016/j.jcomc.2021.100120
21. G. Cheng, L. Geunsik, S. Bin, E. M. Vogel, R. M. Wallace, and C. Kyeongjae, *Appl. Phys.*, **108**: 123711 (2010); https://doi.org/10.1063/1.3524232
22. L. Pei, X. Jingpei, W. Aiqin, M. Dougin, and M. Zhiping, *Appl. Surf. Sci.*, **517**: 146040 (2020); https://doi.org/10.1016/j.apsusc.2020.146040
23. M. Vanin, J. Mortensen, A. K. Kelkkanen, J. M. Garcia-Lastra, K. S. Thygesen, and K. W. Jacobsen, *Phys. Rev. B*, **81**: 081408(R) (2010); https://doi.org/10.1103/PhysRevB.81.081408
24. K. Pi, K. M. McCreary, W. Bao, H. Wei, Y. F. Chiang, Y. Li, S.-W. Tsai, C. N. Lau, and R. K. Kawakami, *Phys. Rev. B*, **80**: 075406 (2009); https://doi.org/10.1103/PhysRevB.80.075406
25. R. Skyner, J. L. McDonagh, C. R. Groom, T. Mourika, and J. B. O. Mitchell, *Phys. Chem. Chem. Phys.*, **17**: 6174 (2015); https://doi.org/10.1039/C5CP00288E
26. R. G. Parr and W. Yang, *Density Functional Theory of Atoms and Molecules* (New York: 1989).
27. W. Koch and M. C. Holthausen, *Chemists Guide to Density Functional Theory* (New York: 2001).
28. A. V. Arbuznikov, *Struct. Chem.*, **48**: S1 (2007); https://doi.org/10.1007/s10947-007-0147-0
29. M. K. Sabbe, M. F. Reyniersa, and K. Reuter, *Catal. Sci. Technol.*, **2**: 2010 (2012); https://doi.org/10.1039/C2CY20261A
30. N. Lopez, N. Almora-Barrios, G.Carchini, B. Piotr, L. Bellarosa, R. García-Muelas, G. Novell-Leruthb, and M. García-Mota, *Catal. Sci. Technol.*, **2**: 2405 (2012); https://doi.org/10.1039/C2CY20384G
31. T. C. Allison and Y. Y. J Tong, *Phys. Chem. Chem. Phys.*, **28**: 12858 (2011); https://doi.org/10.1039/C1CP20376B
32. M. J. Frisch, G. W. Trucks, H. B. Schlegel, G. E. Scuseria, M. A. Robb, J. R. Cheeseman, G. Scalmani, V. Barone, B. Mennucci, G. A. Petersson, H. Nakatsuji, M. Caricato, X. Li, H. P. Hratchian, A. F. Izmaylov, J. Bloino, G. Zheng, J. L. Sonnenberg, M. Hada, M. Ehara, K. Toyota, R. Fukuda, J. Hasegawa, M. Ishida, T. Nakajima, Y. Honda, O. Kitao, H. Nakai, T. Vreven, J. A. Montgomery, Jr., J. E. Peralta, F. Ogliaro, M. Bearpark, J. J. Heyd, E. Brothers, K. N. Kudin, V. N. Staroverov, T. Keith, R. Kobayashi, J. Normand, K. Raghavachari, A. Rendell, J. C. Burant, S. S. Iyengar, J. Tomasi, M. Cossi, N. Rega, J. M. Millam, M. Klene, J. E. Knox, J. B. Cross, V. Bakken, C. Adamo, J. Jaramillo, R. Gomperts, R. E. Stratmann, O. Yazyev, A. J. Austin, R. Cammi, C. Pomelli, J. W. Ochterski, R. L. Martin, K. Morokuma, V. G. Zakrzewski, G. A. Voth, P. Salvador, J. J. Dannenberg, S. Dapprich, A. D. Daniels, O. Farkas, J. B. Foresman, J. V. Ortiz, J. Cioslowski, and D. J. Fox, *Gaussian 16, Revision B.01* (Wallingford CT: Gaussian, Inc.: 2016).
33. G. Schreckenbach, P. J. Hay, and R. L. Martin, *Inorg. Chem.*, **37**: 4442 (1998); https://doi.org/10.1021/ic980057a
34. Georg Schreckenbach, P. Jeffrey Hay, and Richard L. Martin, *Comput. Chem.*, **20**: 70 (1999); https://doi.org/10.1002/(SICI)1096-987X(19990115)20:1<70::AID-JCC9>3.0.CO;2-F
35. A. D. Becke, *Chem. Phys.*, **20**: 70 (1999); https://doi.org/10.1007/PL00021027
36. V. V. Tytarenko, V. A. Zabludovsky, E. Ph. Shtapenko, and I. V. Tytarenko, *Phys. Chem. Solid State*, **23**, No. 3: 461 (2022); https://doi.org/10.15330/pcss.23.3.461-467